Micromechanics-based viscoelasticity predictions of crumb rubber modified bitumen considering polymer network effects

Wang, H.; Zhang, H.; Liu, X.; Apostolidis, P.; Erkens, S.; Scarpas, Athanasios; Leng, Zhen ; Airey, G.D.

Important note
To cite this publication, please use the final published version (if applicable).
Please check the document version above.

Research Article

Micromechanics-Based Viscoelasticity Predictions of Crumb Rubber Modified Bitumen Considering Polymer Network Effects

Haopeng Wang[1,2], Hong Zhang[2], Xueyan Liu[2], Panos Apostolidis[2], Sandra Erkens[2], Athanasios Skarpas[2,3], Zhen Leng[4], and Gordon Airey[1]

Abstract

Crumb rubber modified bitumen (CRMB) can be regarded as a binary composite system in which swollen rubber particles are embedded in the bitumen matrix. Previous study has successfully implemented the micromechanics models in predicting the complex moduli of CRMB binders using more representative constituent parameters. In the regime of master curves, while the micromechanics models used predicted well in the high-frequency range, they underestimated the complex modulus in the low-frequency range. The current study aims to further improve the prediction accuracy of micromechanics models for CRMB by considering the interparticle interactions. To accomplish this goal, a new reinforcement mechanism called chain entanglement effect was introduced to account for the interparticle interaction effect. Results show that the polymer chain entanglement effect accounts for the underestimation of complex modulus and lack of elasticity (overestimation of phase angle) for CRMB at high temperatures/low frequencies. The mechanical properties of bitumen matrix and entangled polymer network can be determined based on the rubber content. The introduction of the entangled polymer network to the generalized self-consistent model significantly improved the prediction accuracy for both complex modulus and phase angle in the whole frequency range. In summary, by incorporating the physio-chemical interaction mechanism into the currently available models, a new dedicated micromechanics model for predicting the mechanical properties of CRMB has been developed. The predicted viscoelastic behaviors can thereafter be used as inputs for an improved mix design.

Keywords

infrastructure materials, asphalt binders, asphalt binder modifiers, asphalt rubber, rheological properties, micromechanics, polymer network

Incorporating crumb rubber from scrap tires into bitumen modification has been a successful engineering practice in the asphalt paving industry. The wet-process crumb rubber modified bitumen (CRMB) was reported to have superior performance characteristics compared with neat bitumen (*1, 2*). To have a proper CRMB binder design, it is essential first to understand the interaction mechanism between rubber and bitumen. After gaining insights into the mechanism, it is also of vital importance to control the interaction process (e.g., temperature and time) and optimize the material parameters (e.g., type of bitumen and rubber, rubber content, morphology, particle size, etc.), with the ultimate goal to

develop CRMBs of desired mechanical properties. The determination of the linear viscoelastic (LVE) properties

[1]Nottingham Transportation Engineering Centre, University of Nottingham, Nottingham, UK
[2]Section of Pavement Engineering, Faculty of Civil Engineering and Geosciences, Delft University of Technology, Delft, the Netherlands
[3]Department of Civil Infrastructure and Environmental Engineering, Khalifa University, Abu Dhabi, United Arab Emirates
[4]Department of Civil and Environmental Engineering, The Hong Kong Polytechnic University, Hong Kong, China

Corresponding Author:
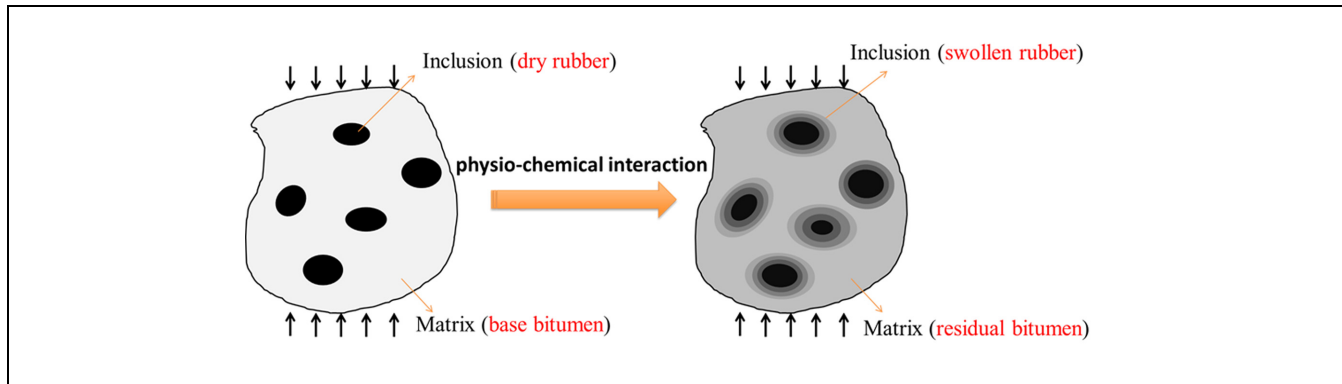Haopeng Wang, haopeng.wang@nottingham.ac.uk

Figure 1. Schematic representation of the RVE of the CRMB composite system before and after interaction.
Note: RVE = representative volume element; CRMB = crumb rubber modified bitumen.

of bituminous materials could operate as a bridge to link chemical composition and performance (_3–5_). In this context, one of the vital issues that need to be addressed is how to effectively predict the performance of modified binders instead of carrying out laboratory work.

Numerical and analytical tools are often used to achieve this goal. Although considerable work has been reported to measure and even predict empirical and fundamental properties of CRMB, very little work has been found in which strict mechanics-based models have been developed to investigate the complicated behavior of CRMB (_6_). Some empirical models were developed to describe the effect of rubber modification on CRMB. These straightforward models are based on the correlations between rubber-related variables (particle size, surface area, etc.) and resultant composite response (_7, 8_), which are incapable of providing generalized insights into the impact of physio-chemical interactions between the constituents. How to adequately address the reinforcement mechanisms in CRMB using micromechanical modeling remains a challenge. Practically speaking, if the predictions of mechanical properties of CRMB from the known properties and blend percentages of the constituent phases by using micromechanics models are applicable and possess certain levels of accuracy, tremendous time and cost can be saved in the laboratory. Such predictions could also enable a more appropriate selection of raw materials (bitumen and rubber type), material development (binder preparation conditions), and design of binders (rubber content and particle gradation) (_9_).

Micromechanics models are capable of predicting fundamental material properties of a composite based on the microstructural description and the local behaviors of its constituents. They have been successfully introduced for predicting the effective viscoelastic behavior of bituminous materials (_10–14_). In particular, CRMB can be regarded as a binary composite in which bitumen is the matrix while rubber particles are the inclusions.

However, the composite system of CRMB is more complicated than asphalt mastic or mixture because of the interaction between rubber particles and bitumen, which alters both the mechanical properties and the volume fractions of individual constituents. To estimate the effective properties of a heterogeneous composite based on the properties and volume fractions of individual constituents, a homogenization theory was developed to derive a homogenized description for the medium based on the assumption of representative volume element (RVE) (_15_). Figure 1 schematically illustrates the RVE of the CRMB composite system before and after interaction (_9_).

After the bitumen–rubber interaction process, the properties of both bitumen and rubber phases have significantly changed. From a micromechanics point of view, the following aspects have been altered: (a) the component proportions and thus the mechanical properties of bitumen matrix as a result of the loss of light fractions and the potential released components from rubber; (b) the mechanical properties of rubber because of the formation of a gel-like structure; (c) the volume content of rubber because of swelling; and (d) the interfacial properties between bitumen and rubber as a result of factors mentioned above (_2, 16_). Thus, the accurate determination of input parameters from constituents is of vital importance and directly affects the accuracy of the model predictions.

Previous studies (_17–19_) have developed dedicated laboratory tests and numerical tools to obtain the input parameters to be implemented in the micromechanics models. Several typical micromechanics models, that is, the dilute model (DM), the Mori-Tanaka (MT) model, the self-consistent (SC) model, and the generalized self-consistent (GSC) model, were used to predict the complex modulus of CRMB binders. It was found that although the four models can give reasonable predictions, GSC has the highest prediction accuracy (_9_). More

importantly, all the micromechanics models predict well in the high-frequency range while yielding biased predictions in the low-frequency range, especially at high rubber contents. Considering that low frequencies correspond to high temperatures in the frame of master curves, rubber particle interaction will be more prominent in CRMB at high temperatures since the bitumen phase is softer. The underestimation of complex modulus at high temperatures is because these models did not explicitly consider the particle interactions (*11*, *13*). All the rubber particles were taken as equivalent inclusions for MT, SC, and GSC. Under this circumstance, the viscoelastic behavior of the composite is dominated by the matrix phase. However, at high temperatures, the rubber inclusion may have more dominant effects on the binder viscoelastic behavior than the bitumen matrix does. The particle's relative configuration and geometrical properties, and their interactions, were not considered. Therefore, to amend the underestimation of the complex modulus of CRMB in the low-frequency range, methods that can more properly address the interparticle interactions should be investigated.

To achieve this goal, a new reinforcement mechanism was introduced to account for the interparticle interaction effect. To this end, the reinforcing effect caused by polymer chain entanglement was added to the current micromechanics models. The constitutive models of this reinforcement were derived based on the difference between experimental data and micromechanics prediction results.

Figure 2. Schematic representations of: (*a*) parabolic dashpot, (*b*) Huet model, (*c*) Huet-Sayegh model, and (*d*) 2S2P1D model.

Linear Viscoelastic Properties of Bituminous Materials

Constitutive Modeling of Linear Viscoelasticity

After obtaining the LVE properties of bitumen matrix and rubber inclusion through Dynamic Shear Rheometer (DSR) tests, the time–temperature superposition principle was applied to build the master curves of complex modulus and phase angle at a particular reference temperature. The master curves can be constitutively modeled by empirical mathematical models and mechanics element models. Many empirical algebraic equations, such as the Christensen and Anderson (CA) model, the Christensen, Anderson and Marasteanu (CAM) model, the polynomial model, the sigmoidal model, the generalized logistic sigmoidal model, and so forth, have been developed to describe the viscoelastic behavior of bituminous materials (*20*). Although mathematical model parameters can be adjusted to fit the experimental data well, they usually lack fundamental physical implications. By contrast, mechanics models represented by a combination of mechanical analogies (i.e., springs and dashpots)
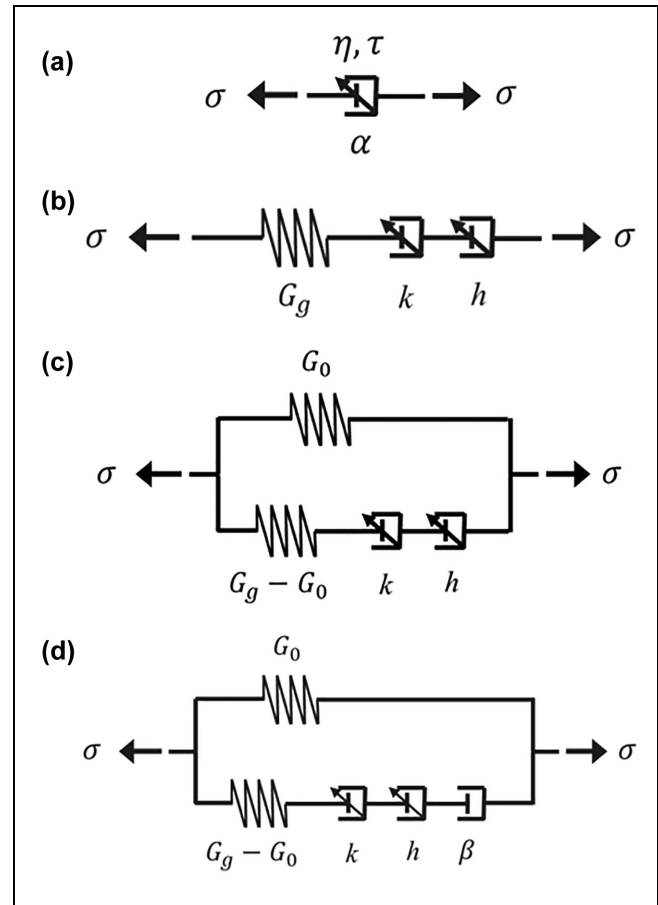
are established through vigorous derivations and can be related to the microstructural features of materials.

Typical mechanics element models include the Maxwell model, Kelvin model, standard linear solid model, Burgers model, generalized Maxwell model, generalized Kelvin model, and so forth (*20*). With an increased number of model elements, the generalized Maxwell model can achieve ideal results in simulating the behavior of viscoelastic liquid-type materials. The generalized Kelvin model is more suitable for simulating viscoelastic solid-type materials. However, with the increase of the number of mechanics elements, the computational efforts in the analysis process will increase significantly (*21*). Thus, to reduce the number of parameters involved, the so-called variable or parabolic dashpot was introduced to replace the linear dashpot to formulate the fractional-order mechanics models. The mechanical response characteristic of the parabolic element is in between those of the linear spring and linear dashpot, as shown in Figure 2*a* (*22*). The addition of the parabolic element improves the ability to describe the LVE properties and provides a continuous spectrum. With the aid of

the parabolic element, several classic models, such as the Huet model, the Huet-Sayegh model, the 2S2P1D model, and so forth, were developed in the past several decades to describe the LVE properties of bituminous materials (23). The arrangements of the mechanical analogies of the above fractional models are shown in Figure 2.

The Huet model consists of a combination of a spring and two parabolic elements (k and h) in series, as illustrated in Figure 2b. The Huet model can be generalized by adding a spring of small rigidity in parallel to form the Huet-Sayegh model. The 2S2P1D model, which stands for two springs, two parabolic elements, and one dashpot, is equivalent to appending a linear dashpot in line with the parabolic dashpots and spring within the Huet-Sayegh model. The analytical expressions of complex modulus of Huet, Huet-Sayegh, and 2S2P1D models are shown in Equations 1 to 3, respectively.

$$G^*(\omega) = \frac{G_g}{1 + \delta(i\omega\tau)^{-k} + (i\omega\tau)^{-h}} \quad (1)$$

where G^* is the complex modulus; ω is the angular frequency; G_g is the glassy modulus when $\omega \to \infty$; h, k are exponents such as $1 > h > k > 0$; δ is a dimensionless constant; i is the complex number; and τ is the characteristic time, which varies with temperature.

$$G^*(\omega) = G_0 + \frac{G_g - G_0}{1 + \delta(i\omega\tau)^{-k} + (i\omega\tau)^{-h}} \quad (2)$$

where G_0 is the static modulus when $\omega \to 0$. If G_0 equals zero, then the Huet-Sayegh model is identical to the Huet model.

$$G^*(\omega) = G_0 + \frac{G_g - G_0}{1 + \delta(i\omega\tau)^{-k} + (i\omega\tau)^{-h} + (i\omega\beta\tau)^{-1}} \quad (3)$$

where η is the Newtonian viscosity, and $\beta = \eta/(G_g - G_0)\tau$ is a dimensionless constant, which can be used for describing the viscous flow of the material.

Generally, the complex modulus, G^*, can be expressed by storage modulus, G', and loss modulus, G'', as follows:

$$G^*(\omega) = G' + iG'' \quad (4)$$

By separating the variables, Equations 2 and 3 can be converted into a form which is analogous to Equation 4, as

$$G^*(\omega) = \left[G_0 + \frac{(G_g - G_0) \times (1 + A)}{(1 + A)^2 + B^2} \right] + \left[\frac{(G_g - G_0) \times (-B)}{(1 + A)^2 + B^2} \right] i \quad (5)$$

For the Huet-Sayegh model, variables A and B are defined as below (24):

$$A(\omega) = \delta(\omega\tau)^{-k} \times \cos\left(\frac{k\pi}{2}\right) + (\omega\tau)^{-h} \times \cos\left(\frac{h\pi}{2}\right) \quad (6)$$

$$B(\omega) = -\delta(\omega\tau)^{-k} \times \sin\left(\frac{k\pi}{2}\right) - (\omega\tau)^{-h} \times \sin\left(\frac{h\pi}{2}\right) \quad (7)$$

For the 2S2P1D model, variable A can be defined as the same as that of the Huet-Sayegh model. However, variable B is defined below (22):

$$B(\omega) = -(\omega\beta\tau)^{-1} - \delta(\omega\tau)^{-k} \times \sin\left(\frac{k\pi}{2}\right) - (\omega\tau)^{-h} \times \sin\left(\frac{h\pi}{2}\right) \quad (8)$$

LVE Property Prediction Framework for CRMB

As emphasized before, from a practical point of view, it is desirable to predict the CRMB LVE properties based on the ingredient properties and recipe. With the mentioned strategy in this study, the LVE property prediction framework for CRMB is illustrated in Figure 3.

As for the micromechanics modeling, the LVE properties of bitumen matrix and rubber inclusion and the volume fraction of rubber must be provided as the input parameters. At a given processing condition (temperature and time) for preparing CRMB, the bitumen matrix properties can be predicted from the base bitumen properties based on the rubber content. The effective rubber volume fraction can be predicted through the finite element (FE) swelling model simulation (18). The constitutive model of the entangled polymer network, which will
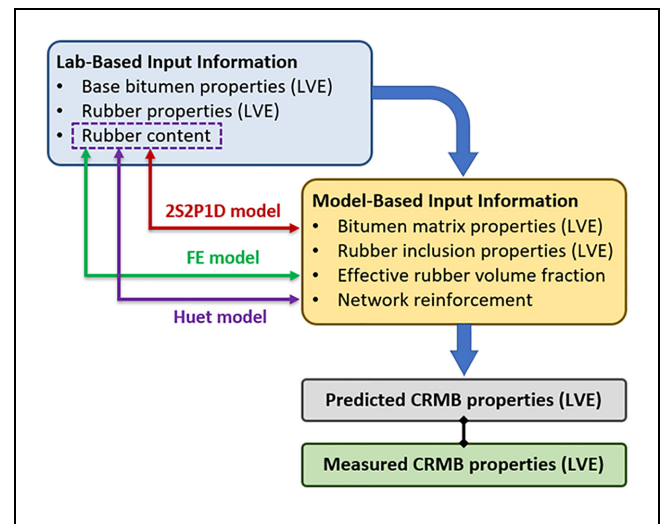
Figure 3. LVE properties determination framework for CRMB.
Note: LVE = linear viscoelastic; CRMB = crumb rubber modified bitumen; FE = finite element.

be used to calibrate the micromechanics model, can also be used to calibrate the micromechanics model, can also be estimated based on the rubber content. At a given condition, rubber inclusion properties depend on the properties of both base bitumen and dry rubber and their physio-chemical interaction. It is difficult to link them together directly, but empirical relationships can be built to predict the rubber inclusion properties. In general, the LVE property prediction framework shown in Figure 3 is feasible and quite promising. After knowing the properties of base bitumen and rubber and the rubber content, the LVE properties of the resulting CRMB at a given processing condition can be estimated with experimental evidence and numerical iterations. The next sections will follow this framework to predict the LVE properties of CRMB.

Input Parameters for Micromechanics Models

Materials and Methods

Penetration grade 70/10 bitumen (Nynas) and crumb rubber (0–0.71 mm) from waste truck tires (Kargro) using ambient grounding process were selected to prepare CRMB binders. The CRMB binders were produced in the laboratory by blending different percentages of crumb rubber modifiers (CRMs) with base bitumen at 180°C for 30 min according to the mixing procedure developed in a previous study (2). Four CRM contents (5%, 10%, 15%, and 22% by mass of base bitumen) were used to prepare CRMBs, labeled as CRMB-5, CRMB-10, CRMB-15, and CRMB-22. To effectively predict the mechanical properties of CRMB with micromechanics models, the LVE properties of both bitumen matrix and rubber inclusion as well as the volume fraction of each phase are required.

Since the nature of both bitumen and rubber phases changed after the bitumen–rubber interaction, dedicated laboratory tests (frequency sweep tests) were performed to obtain the representative properties of the actual bitumen matrix and rubber inclusion in CRMB (17, 19). The bitumen matrix was extracted by filtering the insoluble rubber particles from CRMB with a mesh sieve (0.063-mm) at 163°C. Cylindrical rubber samples ($\Phi \times h = 8 \times 2$ mm) were cut from waste truck tire tread and were soaked in hot bitumen at 180°C for 36 h to prepare the swollen rubber samples to represent the rubber particle phase in CRMB (25). The effective volume content of rubber after swelling was determined by the FE method (17). Combining with the gradation of crumb rubber, the weighted averaged swelling ratio of rubber phase in CRMB was estimated as 3.126. Based on the densities of bitumen and crumb rubber, the effective volume contents of rubber in CRMB-5, CRMB-10, CRMB-15, and CRMB-22 were estimated as 13.40%, 25.69%, 37.02%, and 51.45%, respectively. The Poisson's ratios of bitumen phase and rubber phase were assumed to be 0.49 and 0.45, respectively (26).

LVE Properties of Bitumen Matrix and Rubber Inclusion

Master Curves of LVE Properties. After obtaining the frequency sweep test data, a modified CAM model and the Williams-Landel-Ferry (WLF) equation were used to develop binder LVE master curves (27). By contrast, a generalized logistic function was used to establish the master curves for swollen rubber samples since rubber is not a rheologically simple material (19). The LVE master curves of base bitumen and the liquid phase (bitumen matrix) were plotted at a reference temperature of 30°C in Figure 4 (17). It can be found that the liquid phase of CRMB is stiffer and more elastic than the base bitumen. The loss of light fractions of bitumen absorbed by crumb rubber during the interaction process will increase the proportions of asphaltenes in bitumen, contributing to the increase of stiffness and elasticity (28).

The LVE master curves of dry and swollen rubber samples were plotted at 30°C in Figure 5 (17). It is noteworthy that dry rubber exhibits obvious elastic behaviors in which complex modulus and phase angle are almost frequency independent, while the swollen rubber exhibits obvious viscoelasticity. After the swelling process, a gel-like structure was formed in the swollen rubber sample as a result of the absorption of bitumen components. Therefore, the swollen rubber became softer and more viscous than the dry rubber.
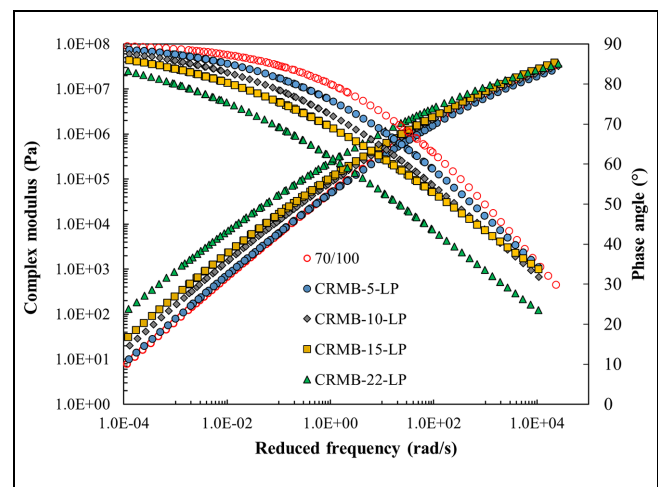

Figure 4. Complex modulus and phase angle master curves of bitumen matrixes.
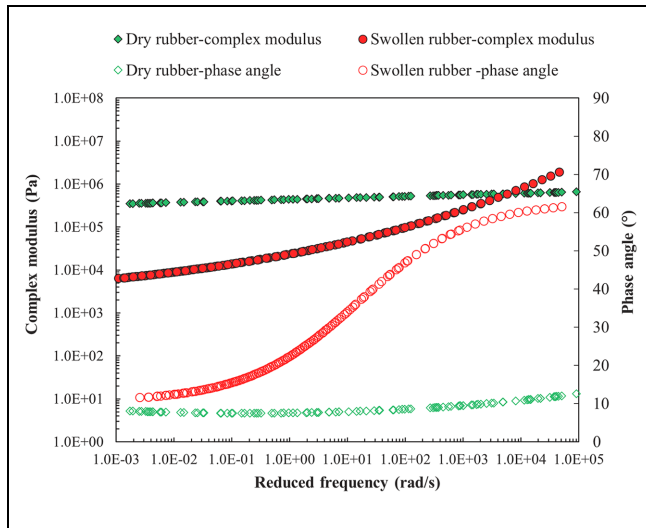*Note*: CRMB = crumb rubber modified bitumen

Figure 5. Complex modulus and phase angle master curves of rubber inclusions.

Constitutive Models of Bitumen Matrix. As pointed out before, the change of the mechanical properties of the CRMB liquid phase has a strong relationship with the rubber content. Therefore, it is desirable to quantitatively relate the rubber content to the constitutive model parameters of the bitumen matrix. Constitutive models were used to model the viscoelastic behavior of the

bitumen matrix since they have fundamental physical meanings. Taking CRMB-22-LP as an example, Figure 6 compares the experimental results with model predictions for both complex modulus and phase angle. The model parameters are summarized in Table 1.

Only the Huet-Sayegh and 2S2P1D models were compared since the Huet model is only a special case of the Huet-Sayegh model. In the model fitting process, the sum of the squared errors for the storage modulus and loss modulus were minimized, as shown in Equation 9.

$$f_{\text{error}} = \sum_{i=1}^{n} \left[\left(\frac{G'_{m,i}}{G'_{e,i}} - 1 \right)^2 + \left(\frac{G''_{m,i}}{G''_{e,i}} - 1 \right)^2 \right] \quad (9)$$

where f_{error} is the sum of the squared errors; $G'_{m,i}$ and $G''_{m,i}$ are storage and loss moduli predicted by the model at the ith frequency, respectively; and $G'_{e,i}$ and $G''_{e,i}$ are storage and loss moduli from experiments at the ith frequency, respectively.

As shown in Table 1, the values of f_{error} for the 2S2P1D and Huet-Sayegh models are 0.035 and 0.136, respectively. From Figure 5, it can also be found that the 2S2P1D model predicts better than the Huet-Sayegh model, especially at very low frequencies. The Huet-Sayegh model has often been reported to describe the rheological properties of asphalt mixes, while the 2S2P1D
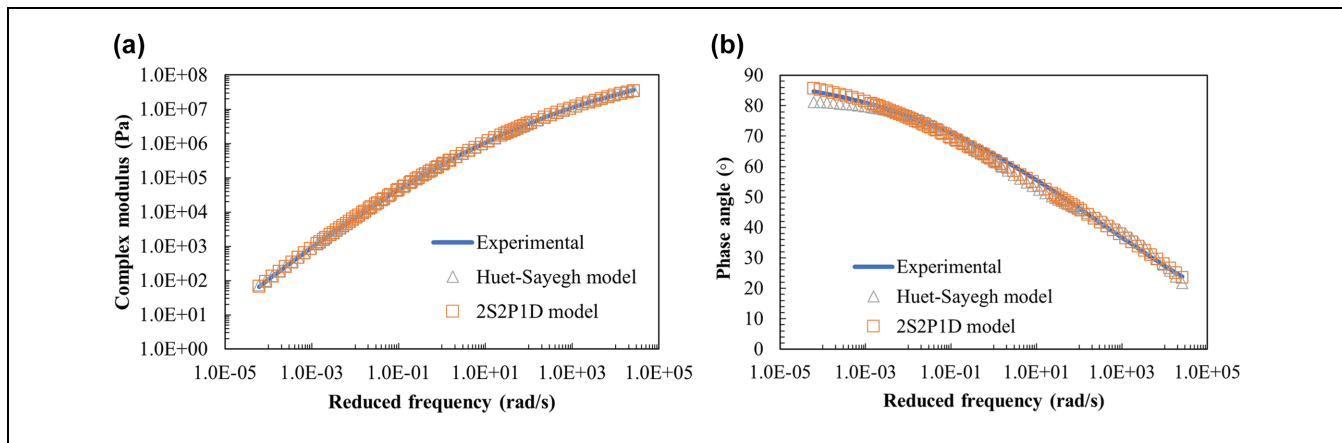

Figure 6. Comparison of Huet-Sayegh model and 2S2P1D model for the LVE properties of CRMB-22-LP: (*a*) complex modulus and (*b*) phase angle.
Note: LVE = linear viscoelastic.

Table 1. Model Parameters for CRMB-22-LP

Model	G_0 (Pa)	G_g (Pa)	k	H	δ	τ	β	f_{error}
Huet-Sayegh	0	6.29E + 07	0.4943	0.9101	10.2923	4.99E−03	na	0.136
2S2P1D	0	8.57E + 07	0.3855	0.7018	3.6941	4.30E−04	35.1501	0.035

Note: CRMB = crumb rubber modified bitumen. na = not applicable.

Table 2. 2S2P1D Model Parameters for CRMB Liquid Phases

Binder type	G_0 (Pa)	G_g (Pa)	k	h	δ	τ	β
70/100	0	1.01E + 09	0.0001	0.6155	13.5173	4.13E−07	194
CRMB-5-LP	0	8.46E + 08	0.0267	0.6211	12.9696	5.13E−07	190
CRMB-10-LP	0	7.67E + 08	0.2397	0.6345	7.2144	1.48E−06	150
CRMB-15-LP	0	2.33E + 08	0.3101	0.6515	2.5400	1.49E−05	83
CRMB-22-LP	0	8.57E + 07	0.3855	0.7018	3.6941	4.30E−04	35

Note: CRMB = crumb rubber modified bitumen.

can be used for both solid asphalt mixes and flowable binders (*20*). Notably, for binders for which G_0 equals zero, the Huet-Sayegh model is equivalent to a parabolic dashpot element while the 2S2P1D model is equivalent to a linear dashpot element at very low frequencies. Binders behave like Newtonian fluids at very low frequencies (very high temperatures), for which a linear dashpot is more suitable than the parabolic dashpot to describe their response. This explains why the 2S2P1D model has better prediction performance than the Huet-Sayegh model.

Relationship between Rubber Content and Model Parameters of Bitumen Matrix. The 2S2P1D model was used for all bitumen matrixes. The constitutive model parameters for each binder are summarized in Table 2, and the correlations between 2S2P1D model parameters and rubber content are presented in Figure 7.

It can be seen from Figure 7 that G_g, δ, and β decrease with the rubber content, while the other three parameters, τ, k, and h, increase with the rubber content. G_g is the glassy modulus at very high frequencies or very low temperatures. It is known that parameters k and h are related to the fractional/variable dashpot. When k or $h \to 0$, the fractional dashpot is equal to a linear spring, while when k or $h \to 1$, the fractional dashpot is equal to a linear dashpot. Parameter τ, which is the characteristic time, is an intrinsic time criterion to characterize the viscoelastic behavior of materials. Here, it denotes the retardation time of the parabolic element in the 2S2P1D model, which is the time delay for the elastic behavior to occur. Thus, with these well-correlated relationships between model parameters and rubber content, it is possible to predict the bitumen matrix properties based on the neat bitumen properties and rubber content.

Micromechanics Models Considering Interparticle Interactions

Strategies for Improving the Micromechanics Prediction Accuracy

It has been discussed that there are three stiffening mechanisms for the CRMB system: the volume-filling effect, physio-chemical interaction, and interparticle interaction (*17*). Volume-filling reinforcement is the stiffening caused by rubber inclusion in the bitumen matrix where the stress/strain fields are disturbed because of the inconsistent mechanical properties of rubber and bitumen. Physio-chemical stiffening is a result of the swelling of rubber in bitumen, which absorbs the bitumen components and increases the effective volume concentration of rubber inclusion. Interparticle interaction is a broad concept. The interparticle interaction effect increases with increasing rubber content in bitumen, as rubber particles may come into contact and form a polymer network. The inability to account for the polymeric network arising from particle interaction was shown by the underestimating of the complex modulus in previous models. In the previous models, the volume-filling reinforcement and the physio-chemical effects were considered (*17*). The interparticle interactions were only partially considered without taking the particle's configuration and interrelation into consideration. Therefore, a new reinforcement mechanism, which brings in the effect of interparticle interaction, will be introduced in the following section.

Viscoelasticity Prediction of CRMB-22 with GSC

It has been pointed out that current micromechanics models underestimated the complex modulus of CRMB at low frequencies or high temperatures. To look into this issue, the GSC model prediction results for CRMB-22 at individual temperatures were compared with the experimental data, as shown in Figure 8. In addition, the phase angle results of CRMB were also compared since the viscoelasticity cannot be defined without considering phase angle. The phase angle is also helpful in understanding the mechanism of the matrix-inclusion interaction at high temperatures.

It can be seen from Figure 8 that both complex modulus and phase angle are generally accurately predicted at low temperatures. With the increase of temperature, underestimating complex modulus was observed, while phase angle prediction results at high temperatures are significantly higher than experimental results. The discrepancy between model prediction and experimental results
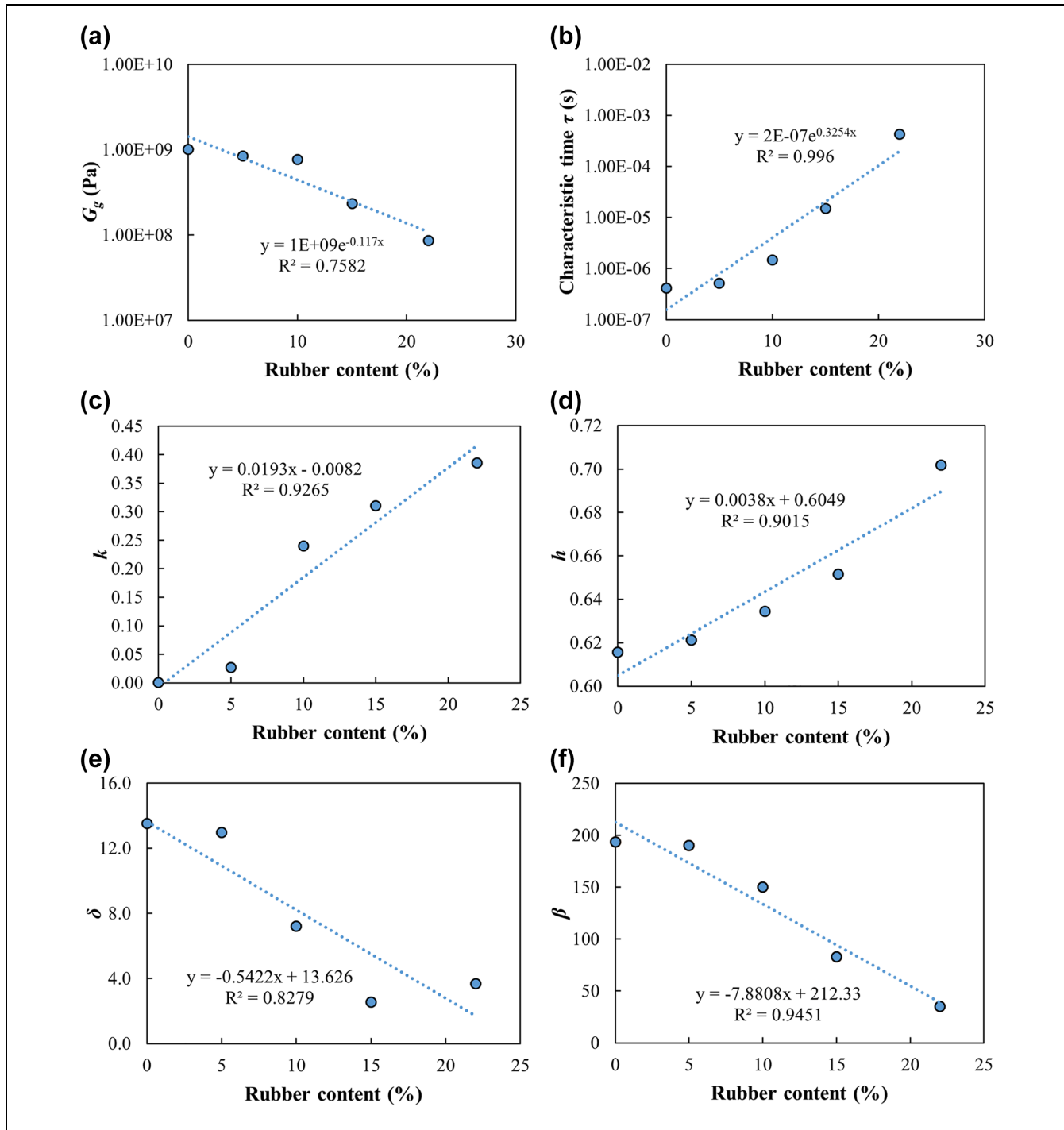
Figure 7. Correlation between 2S2P1D model parameters for bitumen matrixes and rubber content: (*a*) G_g; (*b*) characteristic time τ; (*c*) *k*; (*d*) *h*; (*e*) δ; (*f*) β.

becomes more significant at higher temperatures. Besides, it is noteworthy that the phase angle results of CRMB are atypical compared with unmodified bitumen. It is believed that the presence of rubber particles in the bitumen matrix significantly changes the viscoelastic response of the CRMB binder.

Polymer Chain Entanglement Effect of CRMB System

Reasons for the Inaccurate Predictions for the CRMB System. To address the inaccurate model predictions for the CRMB system, the interrelation between the bitumen matrix and rubber inclusion needs to be carefully analyzed. At low temperatures, the mechanical mismatch
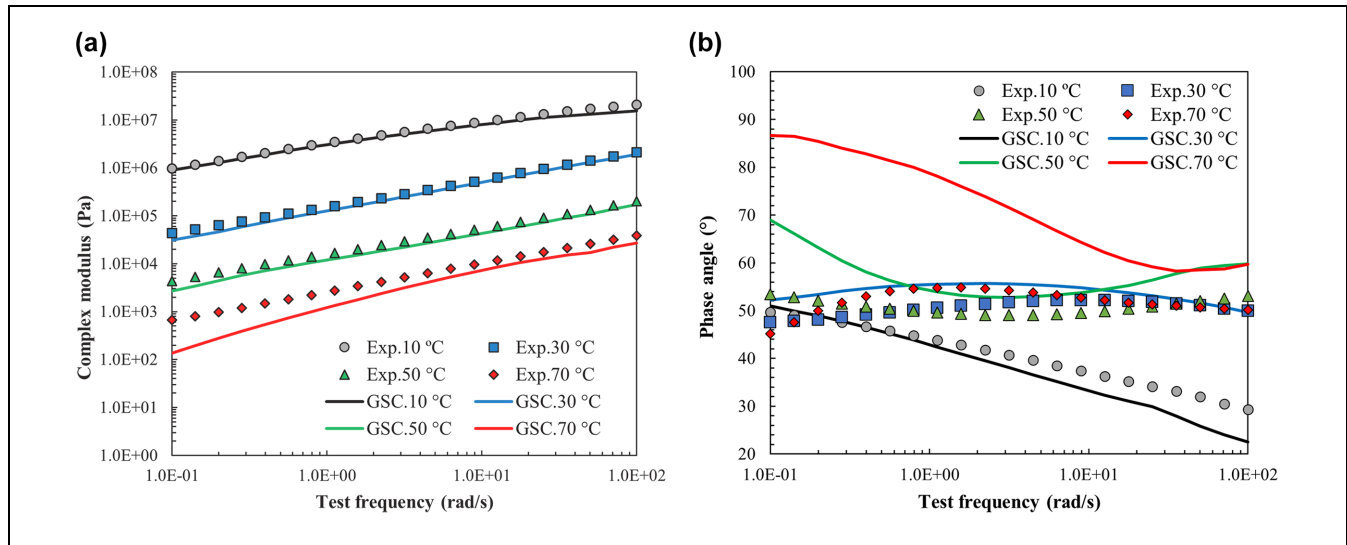
Figure 8. GSC model results for CRMB-22 at each temperature: (*a*) complex modulus and (*b*) phase angle.
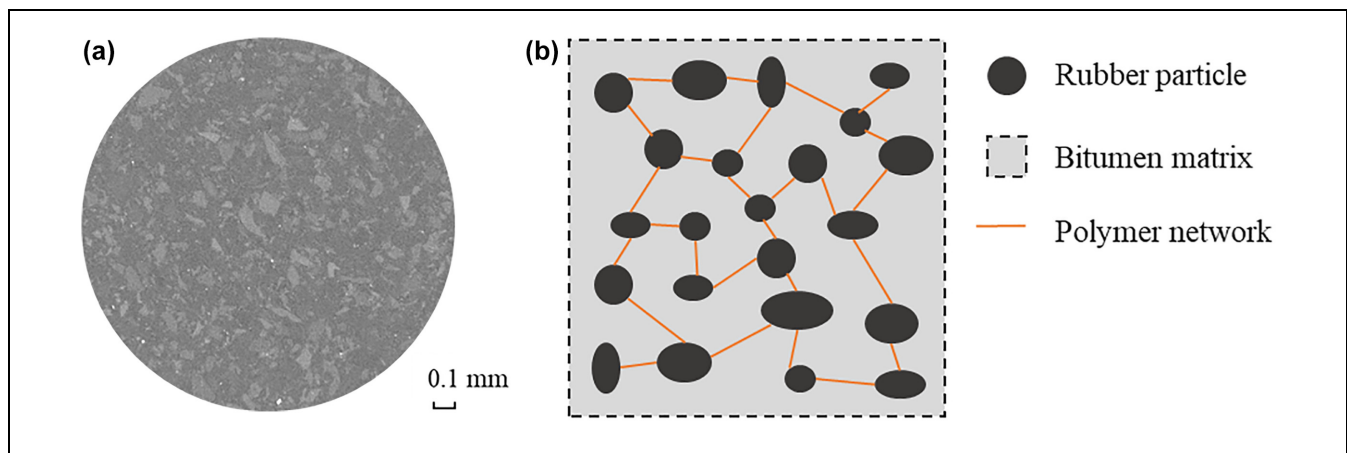*Note*: GSC = generalized self-consistent; CRMB = crumb rubber modified bitumen; exp. = experimental data.

Figure 9. (*a*) CT scan image of CRMB-22. The dark area represents bitumen matrix while the light area represents rubber particles. (*b*) Schematic of polymer network formed by chain entanglement.
Note: CT = computerized tomography; CRMB = crumb rubber modified bitumen.

between rubber particles and bitumen is relatively small, and rubber particles are less active because of the limited polymer chain mobility. Therefore, the micromechanics model prediction results at low temperatures are accurate, even without considering the interparticle interaction effects. However, at high temperatures, the bitumen matrix behaves like a liquid. In contrast, rubber inclusion, which is stiffer than bitumen matrix, will play a more dominant role in determining the mechanical properties of CRMB.

From the computerized tomography (CT) scan image of CRMB-22 in Figure 9*a*, rubber particles are dissociative and do not directly come into contact with each other in the bitumen matrix. Therefore, there is no so-called particle packing effect usually seen in asphalt mixture (*29*). However, recalling the surface layer structure of swollen rubber particles, the disentangled rubber polymer chains on the surface of rubber particles may form a 3-D polymer network (Figure 9*b*) because these disentangled chains from neighboring particles may entangle again (*30*).

Figure 10 illustrates the phenomenon of rubber polymer chain entanglement between two neighboring rubber particles. The improved mobility of disentangled rubber polymer chains at high temperatures will increase chain entanglement chances. Besides, at higher rubber
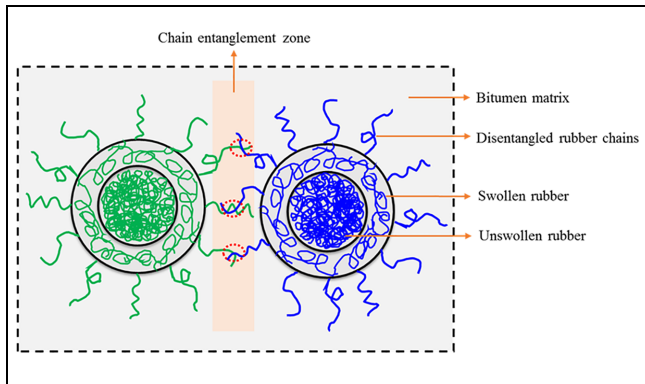
Figure 10. Illustration of rubber chain entanglement. The colors green and blue represent two rubber particles.

concentrations, the chain entanglement effect will be more significant. This potentially formed rubber polymer network resulting from chain entanglement effects will restrain the movement of the dissociative rubber particles, which offers extra elasticity and stiffening effect to the CRMB system, thereby reducing the phase angle and increasing the complex modulus. Therefore, to further improve the prediction accuracy of micromechanics models, a new reinforcement mechanism, which is caused by the chain entanglement effect, must be considered.

Constitutive Models of Entangled Polymer Network. Since polymer chain entanglement occurs at a molecular scale, it is almost impossible to directly measure the mechanical and volumetric properties of the entangled polymer network. Assuming the discrepancy between experiment and micromechanics prediction is originated from the entangled polymer network, the constitutive models of this reinforcement can be derived based on the difference

between experimental data and micromechanics prediction results. The rationale for calibrating the current micromechanics model is adding a network element to the existing model in parallel from a constitutive modeling point of view.

The Huet model was used to fit the mechanical properties of the entangled polymer network based on the difference between experiment and model prediction. The fitted mechanical properties of the entangled polymer network for CRMB with different rubber contents are shown in Figure 11. For comparison, the Huet model fitted results for the dry rubber sample are also plotted in Figure 11.

It can be seen from Figure 11a that the complex modulus curves of the network are merged at high frequencies, which means no significant corrections on the model-predicted complex moduli need to be done at high frequencies. At low frequencies, the original prediction needs significant corrections because of underestimation. For CRMB with a higher rubber content, a stiffer network is required to remedy the underestimation. The complex moduli of both dry rubber and network increase with the frequency.

In addition, with the increase of rubber content, a more elastic (smaller phase angle) network is observed in Figure 11b. It is noteworthy that the phase angle of the entangled network is independent of frequency, which is similar to dry rubber. Compared with the entangled polymer networks, dry rubber is stiffer and more elastic. Generally speaking, the entangled polymer network with a higher rubber content tends to behave like the dry rubber. From the microstructural point of view, dry rubber can be regarded as a much more condensed polymer network than the one considered here. The mechanical similarity between dry rubber and entangled networks
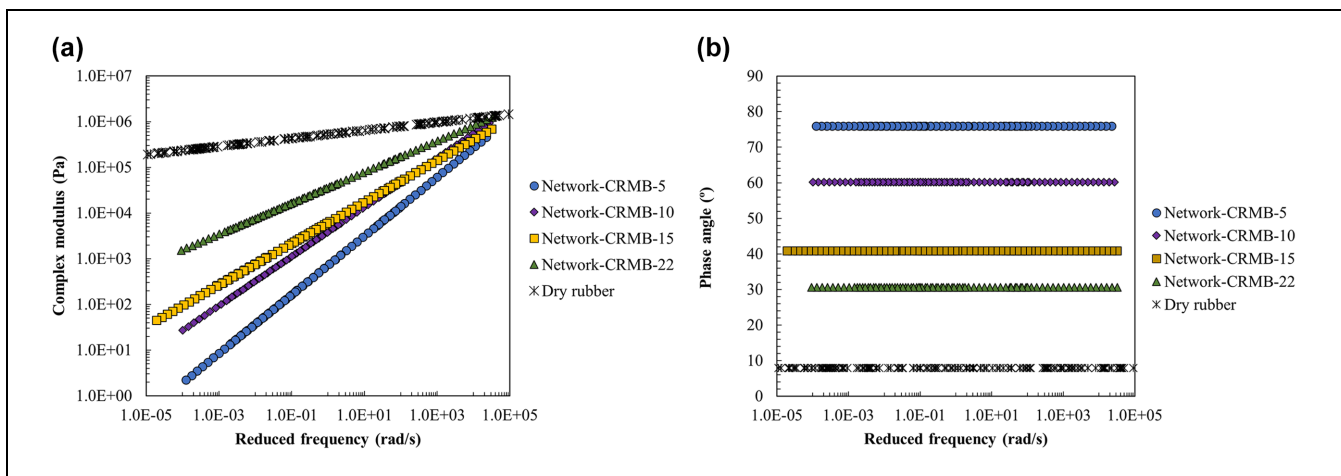

Figure 11. Constitutive models of entangled polymer network (*a*) complex modulus and (*b*) phase angle.
Note: CRMB = crumb rubber modified bitumen.

Table 3. Huet Model Parameters for the Entangled Polymer Network and Dry Rubber

Material	G_g (Pa)	k	h	δ	τ	Phase angle (°)
Network-CRMB-5	1.05E + 10	0.6429	0.6429	4577.3	3.55E−06	75.9
Network-CRMB-10	1.59E + 10	0.5388	0.5388	80378.7	6.65E−04	60.2
Network-CRMB-15	1.86E + 11	0.4541	0.4541	1653891.4	1.70E−03	40.9
Network-CRMB-22	1.91E + 11	0.3404	0.3404	631253.6	1.91E−03	30.6
Dry rubber	1.11E + 11	0.0883	0.0932	82727.0	2.46E−05	7.9

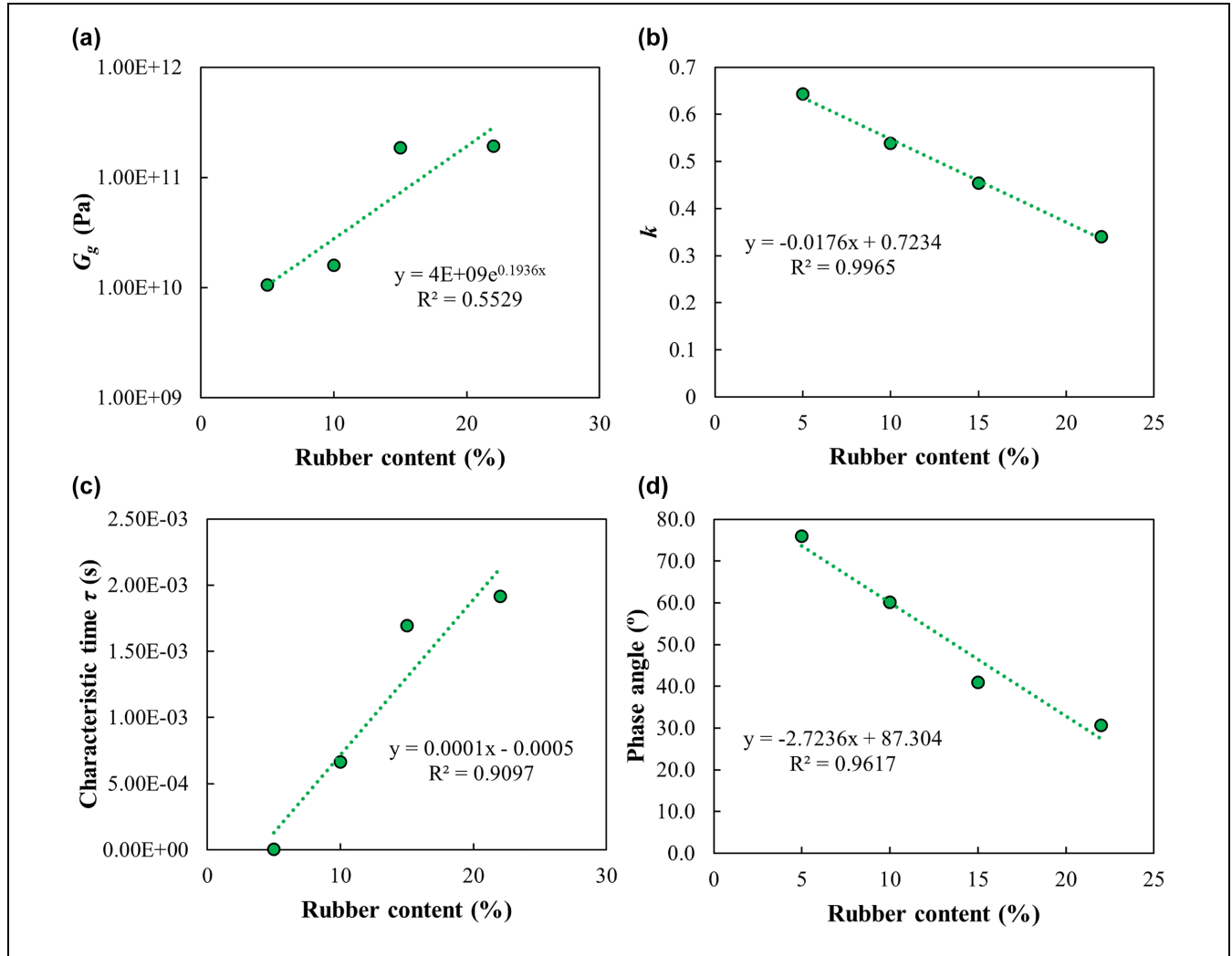*Note*: CRMB = crumb rubber modified bitumen.

Figure 12. Correlation between Huet model parameters for entangled polymer network and rubber content: (*a*) G_g; (*b*) k; (*c*) characteristic time τ; (*d*) phase angle.

implies the possibility of relating the model parameters of networks to that of dry rubber.

Relationship between Rubber Content and Model Parameters of Entangled Polymer Network. Similar to what has been done

to the bitumen matrix, it is also desirable to relate rubber content to model parameters of the entangled polymer network. This is because once these relationships are built, the mechanical properties of networks can be predicted based on the rubber content. Huet model parameters for the entangled polymer network and dry
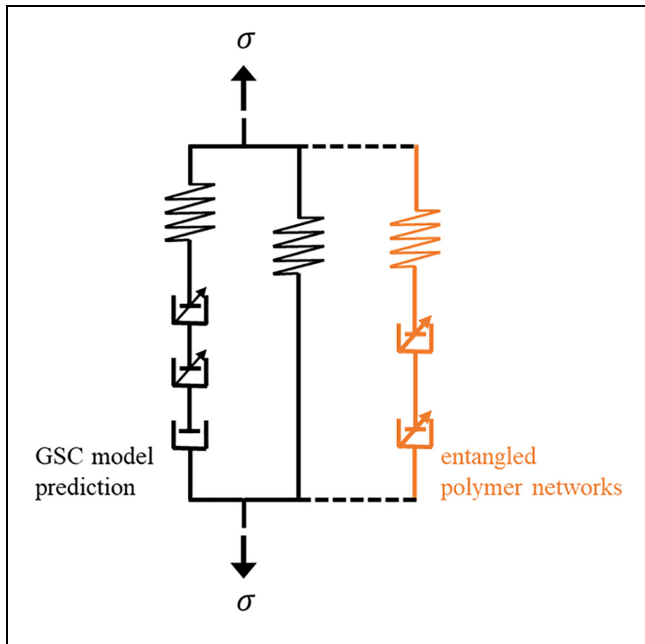
Figure 13. Strategy of considering the network effect on the GSC model predictions.
Note: GSC = generalized self-consistent.

rubber are summarized in Table 3. Since the phase angle of the network is independent of frequency, the phase angle values of different networks are also listed in Table 3 to give a more intuitive comparison. The correlations between model parameters and rubber content are also presented in Figure 12.

It can be seen from Figure 11 that G_g and τ increase with the rubber content, while k, h, and δ decrease with the rubber content. With the increase of rubber content, the entangled network is more elastic, as reflected by the decreased parameters k, h, and δ. It also shows more significant delayed elasticity since the retardation time τ increases. It is noteworthy that parameters k and h of dry rubber are very close to zero, indicating a decisively elastic nature. Although there is a resemblance between the mechanical properties of dry rubber and networks, it is difficult to find quantitative relationships between the model parameters for them because the network and dry rubber are in totally different physical states. Besides, the measured dry rubber sample is filled with carbon black and other additives. It cannot be directly compared with the network, which is supposed to comprise entangled polymer chains. Nevertheless, with the relationships presented in Figure 12, it is possible to predict the mechanical properties of the network based on the rubber content with a certain accuracy.

Calibrated Micromechanics Model Prediction Results

As mentioned before, the strategy of calibrating the current micromechanics model is by adding a network element to the existing model in parallel from a constitutive modeling point of view, as shown in Figure 13. The constitutive elements in black represent the response of the current GSC model, while the constitutive elements in orange represent the additional response from the entangled polymer networks. By integrating these two responses, the current micromechanics model was calibrated.
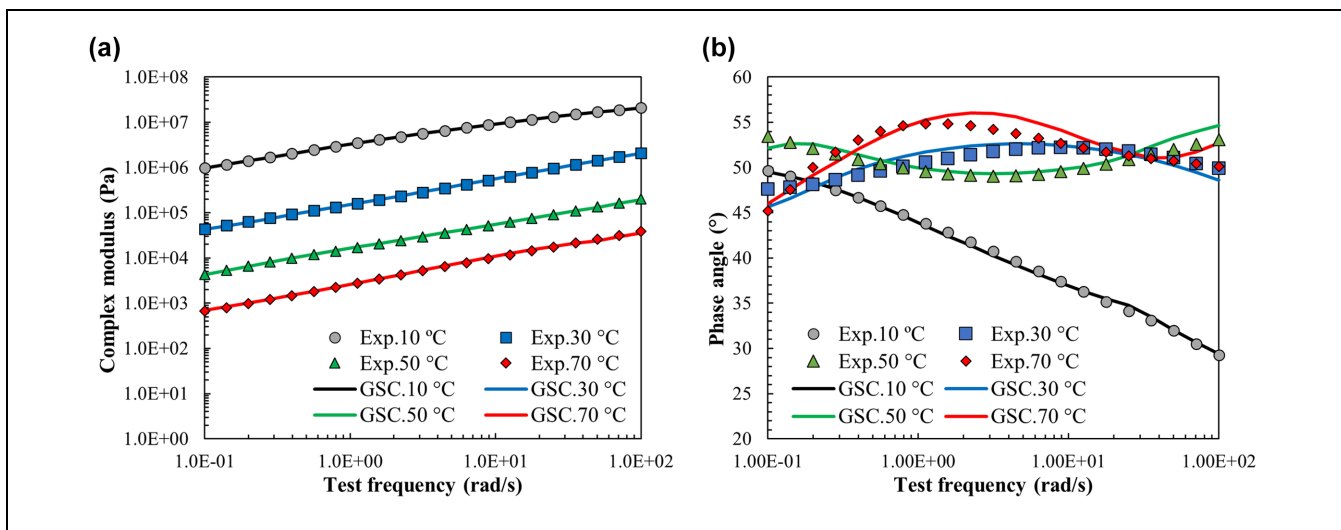

Figure 14. Calibrated GSC model results for CRMB-22 at each temperature: (*a*) complex modulus and (*b*) phase angle.
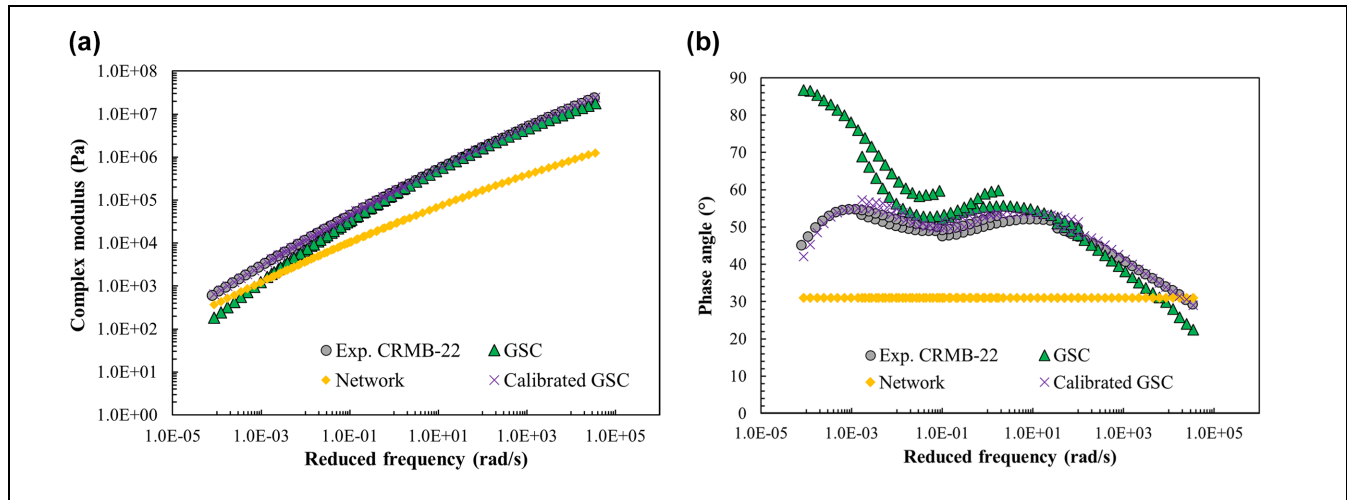*Note*: GSC = generalized self-consistent; CRMB = crumb rubber modified bitumen; exp. = experimental data.

Figure 15. Experimental and model-predicted results for CRMB-22: (*a*) complex modulus and (*b*) phase angle.
Note: CRMB = crumb rubber modified bitumen; exp. = experimental data; GSC = generalized self-consistent model.

Technically, after obtaining the constitutive models of the entangled polymer networks, the extra reinforcement mechanism caused by the chain entanglement effect was added to the current GSC model prediction results through complex number operations. Correspondingly, Figure 14 presents the calibrated GSC model prediction results for CRMB-22 at individual temperatures as an example. Comparing with the original prediction results in Figure 8, the calibrated GSC model significantly improves the prediction accuracy for both complex modulus and phase angle, especially at high temperatures.

Since the prediction accuracy was significantly improved at each temperature by calibrating the GSC model with a network element, it is more convenient to compare the experimental and model prediction results in the framework of the master curve. Figure 15 presents the LVE master curves without smoothing at 30°C from both experiment and model predictions. The atypical pattern of the phase angle master curve of CRMB-22 in the low-frequency range can be noted when comparing with unmodified bitumen. At low frequencies, the phase angle of CRMB-22 first increases and then decreases with increasing frequency. For illustration purposes, the master curves of the entangled polymer network are also plotted to indicate how this extra element can influence the model prediction results. The network element exactly remedies the GSC model prediction inaccuracy, either underestimation or overestimation, at different frequencies. It can be seen from Figure 15*a* that underestimation of complex modulus at low frequencies from the GSC model was rectified after adding the network element. The phase angle master curve predicted from the calibrated GSC model in Figure 15*b* is more accurate after bringing in the elastic element to the original GSC model.

In addition, the calibrated GSC model prediction results for other CRMB binders are shown in Figure 16. As expected, the calibrated GSC model shows superior prediction performance for both complex modulus and phase angle. In summary, there are three main steps involved in the model calibration process:

- ***Step 1.*** Micromechanical prediction using the GSC model based on the bitumen matrix properties and rubber inclusion.
- ***Step 2.*** Fitting the constitutive model of the polymer network based on the difference between GSC predicted data and experimental data.
- ***Step 3.*** Calibration/correction of GSC model by adding the networking element.

Conclusions and Recommendations

This study aimed to further improve prediction accuracy by amending the GSC, which performs best among the current micromechanics models. A new reinforcement mechanism called the chain entanglement effect was introduced to account for the interparticle interaction effect. The main conclusions from the present study can be drawn as follows:

- The polymer chain entanglement effect accounts for underestimating complex modulus and lack of elasticity (overestimation of phase angle) for CRMB at high temperatures/low frequencies.
- The mechanical properties of the bitumen matrix and entangled polymer network can be determined based on the rubber content.
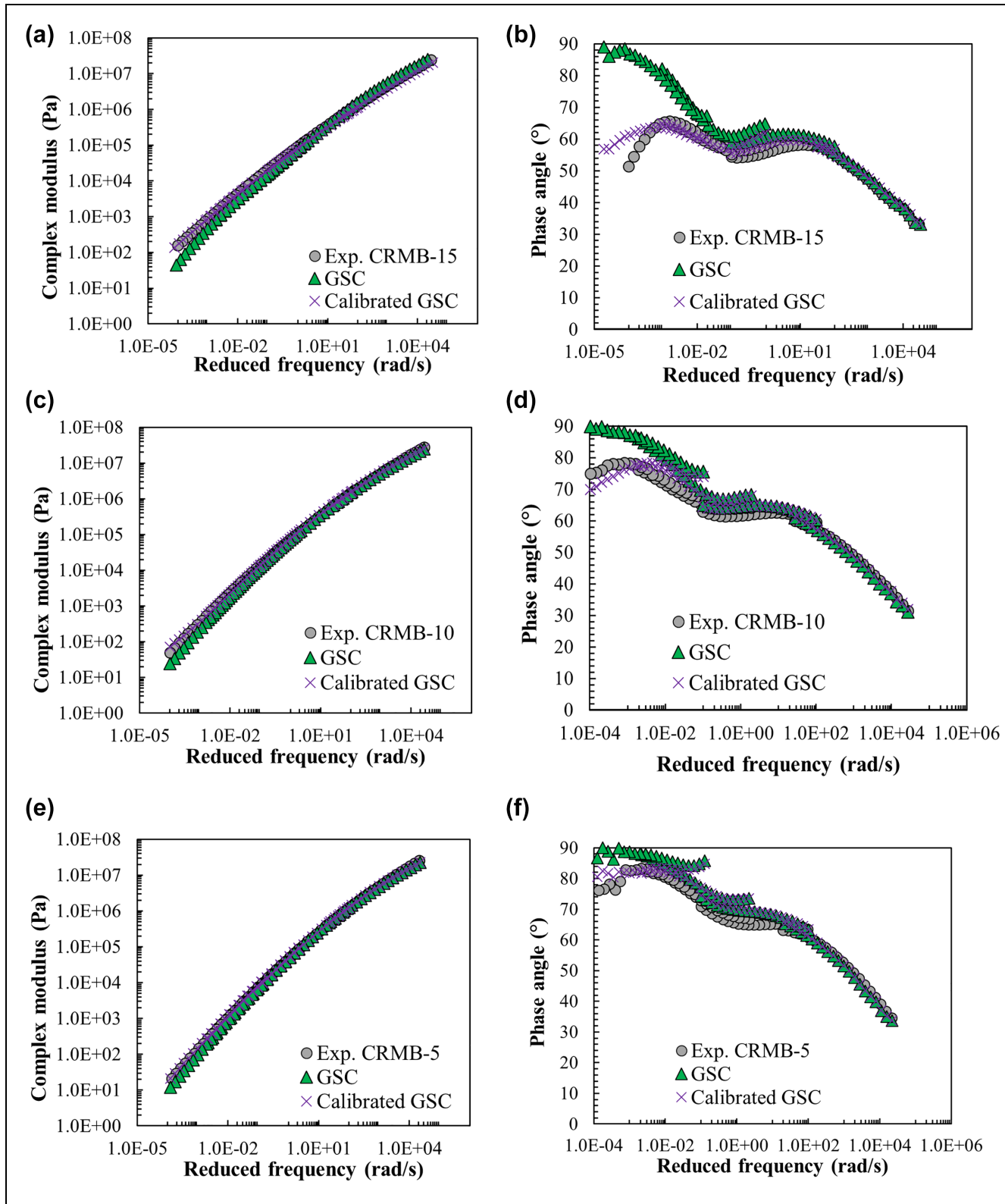- The introduction of the entangled polymer network to the GSC model significantly improved

Figure 16. Experimental and model-predicted results: (*a*) complex modulus of CRMB-15, (*b*) phase angle of CRMB-15, (*c*) complex modulus of CRMB-10, (*d*) phase angle of CRMB-10, (*e*) complex modulus of CRMB-5, and (*f*) phase angle of CRMB-5.
Note: CRMB = crumb rubber modified bitumen; exp. = experimental data; GSC = generalized self-consistent model.

the prediction accuracy for both complex modulus and phase angle in the whole frequency range.

In summary, by incorporating the physio-chemical interaction mechanism into the currently available models, a new dedicated micromechanics model for predicting the mechanical properties of CRMB has been developed. The accurately predicted viscoelastic properties of binders can thereafter be used as binder inputs to improve the performance prediction of the mix, eventually contributing to an improved mix design.

For future studies, mechanics-based efforts can be made to predict the mechanical properties of swollen rubber based on base bitumen and dry rubber properties and their physio-chemical interaction conditions so that the proposed viscoelasticity prediction framework can be more complete. The developed modeling methodology should also be examined by extended binder and rubber sources.

Author Contributions

The authors confirm contribution to the paper as follows: study conception and design: HW, HZ, XL, SE, AS, ZL, GA; data collection: HW; analysis and interpretation of results: HW, HZ, PA; draft manuscript preparation: HW, PA. All authors reviewed the results and approved the final version of the manuscript.

Declaration of Conflicting Interests

The author(s) declared no potential conflicts of interest with respect to the research, authorship, and/or publication of this article.

Funding

ORCID iDs

Haopeng Wang https://orcid.org/0000-0002-5008-7322
Hong Zhang https://orcid.org/0000-0002-9616-2973
Panos Apostolidis https://orcid.org/0000-0001-5635-4391
Zhen Leng https://orcid.org/0000-0002-7797-1134
Gordon Airey https://orcid.org/0000-0002-2891-2517

References

1. Airey, G., M. Rahman, and A. C. Collop. Crumb Rubber and Bitumen Interaction as a Function of Crude Source and Bitumen Viscosity. *Road Materials and Pavement Design*, Vol. 5, No. 4, 2004, pp. 453–475.

2. Wang, H., X. Liu, H. Zhang, P. Apostolidis, T. Scarpas, and S. Erkens. Asphalt-Rubber Interaction and Performance Evaluation of Rubberised Asphalt Binders Containing Non-foaming Warm-Mix Additives. *Road Materials and Pavement Design*, Vol. 21, No. 6, 2020, pp. 1612–1633.

3. Airey, G. D., B. Rahimzadeh, and A. C. Collop. Linear Viscoelastic Limits of Bituminous Binders. *Journal of the Association of Asphalt Paving Technologists*, Vol. 71, 2002, pp. 89–115.

4. Redelius, P., and H. Soenen. Relation between Bitumen Chemistry and Performance. *Fuel*, Vol. 140, 2015, pp. 34–43.

5. Lesueur, D. The Colloidal Structure of Bitumen: Consequences on the Rheology and on the Mechanisms of Bitumen Modification. *Advances in Colloid and Interface Science*, Vol. 145, No. 1–2, 2009, pp. 42–82.

6. Medina, J. R., and B. S. Underwood. Micromechanical Shear Modulus Modeling of Activated Crumb Rubber Modified Asphalt Cements. *Construction and Building Materials*, Vol. 150, 2017, pp. 56–65.

7. Shen, J., S. Amirkhanian, F. Xiao, and B. Tang. Influence of Surface Area and Size of Crumb Rubber on High Temperature Properties of Crumb Rubber Modified Binders. *Construction and Building Materials*, Vol. 23, No. 1, 2009, pp. 304–310.

8. Shen, J., S. Amirkhanian, F. Xiao, and B. Tang. Surface Area of Crumb Rubber Modifier and Its Influence on High-Temperature Viscosity of CRM binders. *International Journal of Pavement Engineering*, Vol. 10, No. 5, 2009, pp. 375–381.

9. Wang, H., H. Zhang, X. Liu, A. Skarpas, S. Erkens, and Z. Leng. Micromechanics-Based Complex Modulus Prediction of Crumb Rubber Modified Bitumen Considering Interparticle Interactions. *Road Materials and Pavement Design*, Vol. 22, 2021, pp. S251–S268.

10. Buttlar, W., D. Bozkurt, G. Al-Khateeb, and A. Waldhoff. Understanding Asphalt Mastic Behavior through Micromechanics. *Transportation Research Record: Journal of the Transportation Research Board*, 1999. 1681: 157–169.

11. Yin, H. M., W. G. Buttlar, G. H. Paulino, and H. D. Benedetto. Assessment of Existing Micro-Mechanical Models for Asphalt Mastics Considering Viscoelastic Effects. *Road Materials and Pavement Design*, Vol. 9, No. 1, 2008, pp. 31–57.

12. Underwood, B. S., and Y. R. Kim. A Four Phase Micro-Mechanical Model for Asphalt Mastic Modulus. *Mechanics of Materials*, Vol. 75, 2014, pp. 13–33.

13. Zhang, H., K. Anupam, A. Scarpas, and C. Kasbergen. Comparison of Different Micromechanical Models for Predicting the Effective Properties of Open Graded Mixes. *Transportation Research Record: Journal of the Transportation Research Board*, 2018. 2672: 404–415.

14. Zhang, H., K. Anupam, T. Scarpas, C. Kasbergen, S. Erkens, and L. Al Khateeb. Continuum-Based Micromechanical Models for Asphalt Materials: Current Practices & Beyond. *Construction and Building Materials*, Vol. 260, 2020, p. 119675.

15. Charalambakis, N. Homogenization Techniques and Micromechanics. A Survey and Perspectives. *Applied Mechanics Reviews*, Vol. 63, No. 3, 2010, p. 030803.

16. Zhu, J., R. Balieu, and H. Wang. The Use of Solubility Parameters and Free Energy Theory for Phase Behaviour of Polymer-Modified Bitumen: A Review. *Road Materials and Pavement Design*, Vol. 22, No. 4, 2019, pp. 757–778.

17. Wang, H., X. Liu, H. Zhang, P. Apostolidis, S. Erkens, and A. Skarpas. Micromechanical Modelling of Complex Shear Modulus of Crumb Rubber Modified Bitumen. *Materials & Design*, Vol. 188, 2020, p. 108467.

18. Wang, H., X. Liu, P. Apostolidis, S. Erkens, and T. Scarpas. Numerical Investigation of Rubber Swelling in Bitumen. *Construction and Building Materials*, Vol. 214, 2019, pp. 506–515.

19. Wang, H., X. Liu, P. Apostolidis, S. Erkens, and A. Skarpas. Experimental Investigation of Rubber Swelling in Bitumen. *Transportation Research Record: Journal of the Transportation Research Board*, 2020. 2674: 203–212.

20. Yusoff, N. I. M., M. T. Shaw, and G. D. Airey. Modelling the Linear Viscoelastic Rheological Properties of Bituminous Binders. *Construction and Building Materials*, Vol. 25, No. 5, 2011, pp. 2171–2189.

21. Park, S. W., and R. A. Schapery. Methods of Interconversion between Linear Viscoelastic Material Functions. Part I: A Numerical Method Based on Prony Series. *International Journal of Solids and Structures*, Vol. 36, No. 11, 1999, pp. 1653–1675.

22. Olard, F., and H. Di Benedetto. General "2S2P1D" Model and Relation between the Linear Viscoelastic Behaviours of Bituminous Binders and Mixes. *Road Materials and Pavement Design*, Vol. 4, No. 2, 2003, pp. 185–224.

23. Wu, Q., C. Wang, R. Liang, Y. Liu, J. Cheng, and Y. Kang. Fractional Linear Viscoelastic Constitutive Relations of Anhydride-Cured Thermosetting Rubber-Like Epoxy Asphalt Binders. *Construction and Building Materials*, Vol. 170, 2018, pp. 582–590.

24. Pronk, A. C. The Huet-Sayegh Model: A Simple and Excellent Rheological Model for Master Curves of Asphaltic Mixes. *Proc., R. Lytton Symposium on Mechanics of Flexible Pavements*, Baton Rouge, Louisiana, 2005.

25. Wang, H., X. Liu, P. Apostolidis, D. Wang, Z. Leng, G. Lu, S. Erkens, and A. Skarpas. Investigating the High- and Low-Temperature Performance of Warm Crumb Rubber–Modified Bituminous Binders Using Rheological Tests. *Journal of Transportation Engineering, Part B: Pavements*, Vol. 147, No. 4, 2021, p. 04021067.

26. Aurangzeb, Q., H. Ozer, I. L. Al-Qadi, and H. H. Hilton. Viscoelastic and Poisson's Ratio Characterization of Asphalt Materials: Critical Review and Numerical Simulations. *Materials and Structures*, Vol. 50, No. 1, 2016, pp. 1–12.

27. Wang, H., X. Liu, P. Apostolidis, and T. Scarpas. Rheological Behavior and Its Chemical Interpretation of Crumb Rubber Modified Asphalt Containing Warm-Mix Additives. *Transportation Research Record: Journal of the Transportation Research Board*, 2018. 2672: pp. 337–348.

28. Apostolidis, P., X. Liu, C. Kasbergen, and A. T. Scarpas. Synthesis of Asphalt Binder Aging and the State of the Art of Antiaging Technologies. *Transportation Research Record: Journal of the Transportation Research Board*, 2017. 2633: 147–153.

29. Zhang, H., K. Anupam, A. Scarpas, C. Kasbergen, and S. Erkens. Effect of Stone-on-Stone Contact on Porous Asphalt Mixes: Micromechanical Analysis. *International Journal of Pavement Engineering*, Vol. 21, No. 8, 2019, pp. 990–1001.

30. Rubinstein, M., and R. H. Colby. *Polymer Physics*. Oxford University Press, New York, NY, 2003.